Solid Freeform Fabrication 2022: Proceedings of the 33rd Annual International Solid Freeform Fabrication Symposium – An Additive Manufacturing Conference
Reviewed Paper

EFFECTS OF SPHERICAL FILLERS ON THE PROCESSABILITY AND MECHANICAL PROPERTIES OF PA613 AND PP-BASED LASER SINTERING DRY BLENDS

I. Kletetzka*, R. Gawlikowicz*, H.-J. Schmid*

* Direct Manufacturing Research Center (DMRC) and Particle Technology Group, Paderborn University, Germany

Abstract

Polymer materials filled with particles may show substantially altered mechanical properties. Therefore, it is an important aim to be able to tailor the mechanical properties of LS components by adding fillers and thus to create new application areas for additively manufactured components. In this work, the influences of spherical fillers on the processing properties and the resulting mechanical properties of laser-sintered components are investigated. For this purpose, micro glass spheres, hollow glass bubbles and mineral spheres are dry blended to the matrix polymers polyamide 613 and polypropylene with filling ratios of 20 and 40 vol%. First, relevant properties of the blends, such as powder flowability, thermal behavior and melt viscosity, are investigated. Based on the results, processing parameters are then developed for the laser sintering (LS) process and the mechanical properties of the components are investigated.

Introduction

Additively manufactured components are increasingly used as functional prototypes or as end user products [1, 2]. In the field of plastics, selective laser sintering appears to be particularly interesting for this purpose, as it enables the production of complex geometries without the use of support while offering a comparatively high productivity [3]. In selective laser sintering, thermoplastic powder is deposited in layers, preheated and selectively melted by a laser to form plastic components. For producing end user products, functional and mechanical properties of additively manufactured components are becoming more important. However, currently there is only a limited selection of LS materials available, meaning that not all customer-specific requirements can be met [2]. Particularly in the automotive and aerospace industries, filled plastics represent standard materials, as they can exhibit better mechanical properties, higher heat resistance or improved wear properties, depending on the filler [4, 5].

In order to create new fields of application for selective laser sintering, the material variety should be extended by filled variants (dry blends) of polypropylene (PP) and polyamide 613 (PA613) within this work. For this purpose, the influence of different fillers and the filling ratio on the mechanical properties will be analyzed, thus enabling application specific tailoring of material properties. The main goal here is an increase in component stiffness while maintaining reasonably good elongation at break and tensile strength. The aim is to not only increase the component stiffness in the dry state, but also after conditioning the test specimens.

The term filler covers a wide range of materials. Fillers are defined by various authors as natural or synthetic particles that do not dissolve in the base polymer and are not volatile [5–7]. Consequently, a matrix is formed of polymer and disperse filler particles with distinct interfaces. The particle shape of the filler can be either spherical, acicular, flakey, fibrous or irregular. At current state of the art, there are essentially three different methods for producing filled powders for the LS process. These methods differ significantly in the properties of the powders produced and in the effort required to produce the respective powders. So far, there are only relatively sparse data available comparing the powders and the resulting component properties of the different manufacturing methods and regarding the impact of different fillers in general. [4, 8–15]

The easiest method for creating filled SLS powders is dry blending. Polymer particles and filler particles are mechanically mixed, for example in a drum hoop mixer or a rotary mixer. Different authors used mixing times in the range of 30 min up to 24 h [10, 13]. With dry blending, a commercially available plastic powder can be quickly mixed with different fillers and filling ratios, allowing the material to be adapted to a specific build job. A possible disadvantage of dry blending is an inhomogeneous distribution of the filler in the polymer powder. Especially if polymer and filler particles differ strongly in morphology and density, the preparation of a homogeneous blend and preventing segregation upon processing is challenging. In addition, the adhesion of filler particles and polymer matrix is based solely on pressure less coalescence in the build process. [15]

An alternative method is the production of filled SLS powder by melt compounding and subsequent cryogenic milling to form a powder. The achievable particle size distribution is often wide and sieving or other classification processes are necessary after milling. Furthermore, the particles tend to have rough surfaces and a very irregular morphology leading to a poor powder flowability. An additional rounding process or the addition of flow improving additives might be necessary. Another challenge is that during the grinding process, separation of the polymer and filler, or comminution of the filler, can take place. [3, 11, 14, 16, 17]

The production of a filled LS powder via thermally induced phase separation (TIPS) aims to create particles in which the filler is completely coated with plastic. Advantages are, that the generated powder usually exhibits a good flowability. However, the process is complex and requires precise control of the process parameters to achieve the desired powder properties. Furthermore, the use of solvents at high temperatures can only be realized with considerable effort in terms of occupational safety and environmental protection. [8, 18]

Materials

The intended approach is to produce a filled material by dry blending various combinations of commercially available polymer powders and fillers. Consequently, the materials must already be available in powder form with an appropriate particle size distribution. Polypropylene (PP 01 nat by BASF) and Polyamide 613 (VESTOSINT 3D 8754HT1 by Evonik) are selected as base polymers for the dry blends. For these polymers, the properties of dry blends have not been studied systematically. Furthermore, PA613 offers better mechanical properties without a filler when compared to PA12. PP has the advantage, that it absorbs almost no moisture and the effects of moisture exposure on mechanical properties should therefore be minimal [19, 20].

This work focuses on spherical fillers, since fibrous fillers proved to cause high anisotropy when used in dry blends for laser sintering and can furthermore decrease the powder flowability [21–23]. Three different spherical fillers with suitable particle size distributions were chosen: glass beads manufactured by Sigmund Lindner (Silibeads 40-70 [24]), glass bubbles manufactured by 3M (iM16k [25]) and mineral beads manufactured by Itochu Ceratech (Naigai Cerabeads #1700 [26]). The Silibeads are made of recycled soda lime glass (A-glass) and have a density of 2.5 g/cm³. 3M glass bubbles are also made from soda lime glass but due to being hollow, their apparent density is only 0,46 g/cm^3. The isostatic crush strength of iM16K is 110 MPa. Naigai Cerabeads are made of sintered mullite and have a density of 2,9 g/cm^3. Both glass fillers were ordered with a silane coating recommended by the manufacturer for the used polymers and without coating. For Silibeads a gamma-aminopropyltriethoxysilane coating with the designation Si-3 was selected, for iM16K the coating was not specified by the manufacturer.

The polymer powders and fillers were mixed using a drum hoop mixer. Each dry blend was mixed for 30 min at a rotational speed of 30 rpm. Since the selected fillers differ considerably in terms of density, the filler content is given in percent by volume. This allows the best possible comparability of the results between the individual filler types. PA613 und PP are blended with the different fillers (with and without silane coatings) in filling ratios of 20 vol% and 40 vol% as listed in table 1. Additionally, all tests are carried out with the unfilled polymers for comparison.

Table 1: Overview of the investigated dry blends

	Polyamide 613 (VESTOSINT 3D 8754HT1)	**Polypropylene (Ultrasint PP 01 nat)**
Glass beads (Silibeads) uncoated and silane coated	0 / 20 / 40 vol%	0 / 20 / 40 vol%
Glass bubbles (iM16K) uncoated and silane coated	0 / 20 / 40 vol%	0 / 20 / 40 vol%
Mullite beads (Cerabeads) uncoated	0 / 20 / 40 vol%	0 / 20 / 40 vol%

Experimental Methods

Before the effect of the fillers on the mechanical properties of laser-sintered components can be identified, suitable parameters must first be developed in order to process the respective blends. For this purpose, the methodology shown in figure 1 was used.

Preliminary tests are carried out on the powder to characterize the impact of different fillers on the powder properties. Subsequently the parameter development on the SLS Systems was carried out. Here, the parameter sets for unfilled polymer powders were used as a starting point. The specimens built with varying laser energy are used to analyze the mechanical properties, part resolution and density. The results are used to determine a feasible laser energy density.

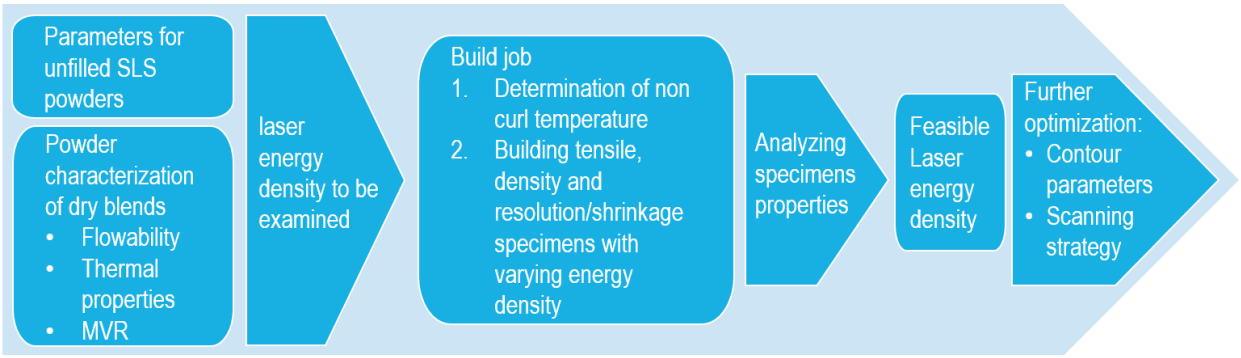

Figure 1: Methodology for parameter development for dry blends

For studying the particle morphology, a Phenom World **scanning electron microscope** (SEM) was used, which allows magnification up to 24,000 times. Beforehand, the samples were sputtered to create the electrical conductivity required for SEM imaging.

The **particle size distribution** was analyzed using dynamic image analysis for moving particles according to ISO 13322-2. The measurements were carried out with a QICPIC manufactured by Sympatec, equipped with a dry dispersion unit. The set measuring range was M5, allowing the detection of particles with a size in between 1,8 and 3755 µm. [27]

The flowability of the powder and mixtures was evaluated by means of the **Hausner ratio** HR. The description of the Hausner ratio is given in VDI 3405 Sheet 1.1. The ratio is defined as the quotient of the tapped density and the bulk density. For measuring, a cylinder was filled up to the 250 ml mark with the powder mixture to be tested, before the powder was deagglomerated in a plastic bag. The measuring cylinder was then closed and tapped uniformly with low force onto a solid surface at a frequency of 0.5 Hz for a duration of two minutes. The process is then repeated with a duration of one minute until the tapping volume no longer changed. To improve the measurement accuracy, the Hausner factor was determined three times for each data point and the mean value was calculated. [28]

The thermal behavior of the dry blends was investigated by **differential scanning calorimetry (DSC)** according to DIN EN ISO 11357-3. A DSC 214 Polyma from Netzsch was used as the measuring instrument. In DSC analysis, small sample quantities (5±0.3 mg) are heated up to a defined temperature and cooled down again, whereby the heat flow between the sample and an empty reference crucible is continuously measured and recorded. During the investigations, the samples were heated up to 250 °C at a heating and cooling rate of 10 K/min. [29]

For the determination of the **melt volume-flow rate (MVR)**, a capillary rheometer of the manufacturer Zwick Roell is used. The test procedure is described in DIN EN ISO 1133-1. Thus, the material to be tested is filled into a cylinder which is heated and melted with a duration of 5 minutes. A piston loaded with a weight generates a pressure which forces the melt through an extrusion nozzle. Before testing, the powder samples were dried in a laboratory oven for 30 min at 105°C to avoid bubble formation and hydrolysis. The test temperature for PA613 powder blends was 240 °C. For PP powder mixtures, the test temperature was set to 220 °C. For all MVR measurements, a weight of 5 kg was used. For each blend, a minimum of three tests was carried out and the average MVR value was calculated. [30]

For the **density measurement** of the sintered components, cubes measuring 20 x 20 x 20 mm were built and tested using the Archimedes principle, which is standardized by DIN EN ISO 1183-1. A sample attached to a wire is first weighed in air and then in ethanol. For this purpose, a precision scale from Sartorius with the model name CPA224S and the associated set for density determination with the name YDK01 was used. For each parameter set, the average density was calculated using three test specimens. [31, 32]

Tensile tests according to DIN 527 were performed to determine the mechanical properties such as modulus of elasticity, tensile strength and elongation at break. For this purpose, laser sintered specimens of type 1A and universal testing machines of type Instron 5569 and Zwick Roell Z2020 were used. The test speed for determining the modulus of elasticity is 1 mm/min and is then increased to 50 mm/min at an elongation at 0.25 % until fracture. In contradiction to the material standard for polyamide and polypropylene, both unreinforced and filled materials are tested at 50 mm/min to ensure the best possible comparability. For every parameter set, average mechanical properties were calculated using 5 test specimens. [33–35]

The mechanical properties of polyamides are strongly dependent on the moisture content in the material, therefore a precise adjustment of this value is necessary to obtain comparable measurements. Tensile properties were therefore evaluated in the dry state and after conditioning. Due to time constraints, accelerated conditioning according to DIN EN ISO 1110 was carried out in a climatic chamber at 70 °C and 62 % relative humidity. To prevent the absorption of moisture in the dry state specimens, they were kept dry in a plastic bag with silica gel pads after the build job until the tensile test was performed. [36]

Powder Characterization

The size, shape and the surface of powder particles have a decisive influence on the powder behavior during the SLS process. If the powder particles have an irregular shape or rough surfaces, the flowability of the powder decreases, since the adhesive forces between the individual particles increase. At the same time, the packing density of the powder decreases. Poorer powder flowability can lead to uneven coating during the powder application process, and reduced powder bed density can lead to pores and a decrease in the mechanical strength. Moreover, the particle size distribution has an influence on the surface quality and the detail resolution of the final part. A high proportion of large powder particles has a negative effect on both properties. An excessive fine powder content, however, has a negative effect on flowability and pourability [3, 37].

The first filler considered is uncoated glass beads named Silibeads. The SEM picture shows, that Silibeads have a very smooth particle surface (figure 2). Most of the particles have a spherical shape, but some irregular particles are present. In addition, some small particles are partially molten into the surface of larger particles. The average sphericity of the particles is 0.852. Silibeads have a relatively narrowly distributed particle size between about 25 µm and 100 µm. In terms of particle morphology and particle size distribution, the Silibeads should be suitable as a filler for the laser sintering polymer powders. Silibeads with a silane coating showed no obvious differences in terms of particle size distribution and particle morphology.

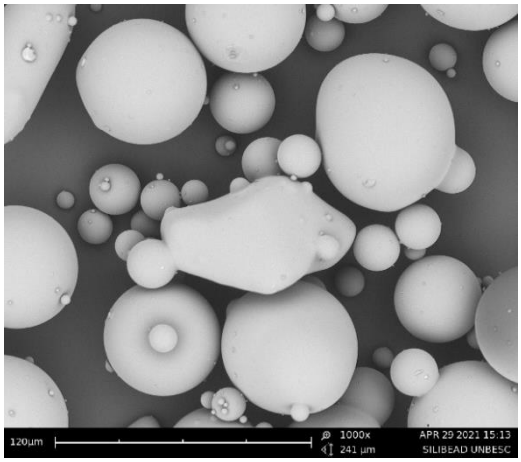

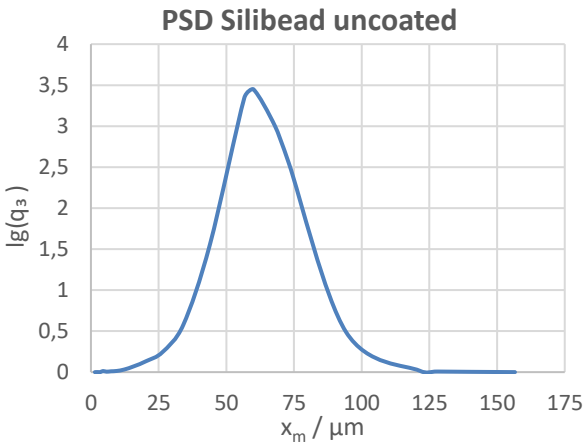

Figure 2: Silibeads uncoated. SEM Picture on the left and particle size distribution on the right

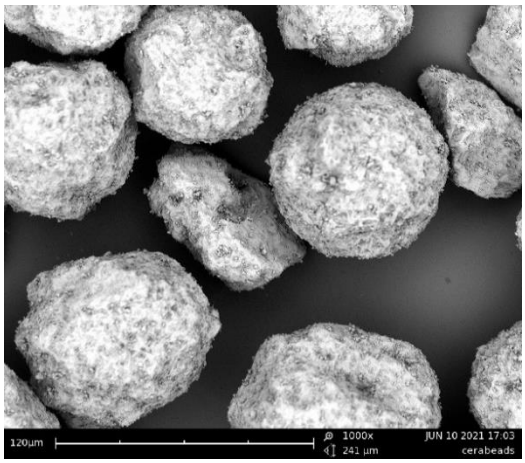

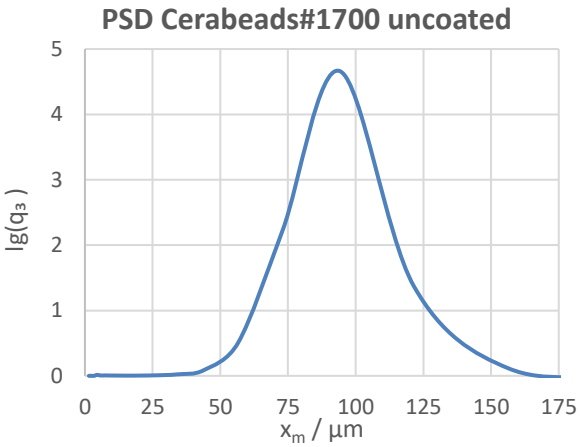

Figure 3: Cerabeads#1700. SEM Picture on the left and particle size distribution on the right

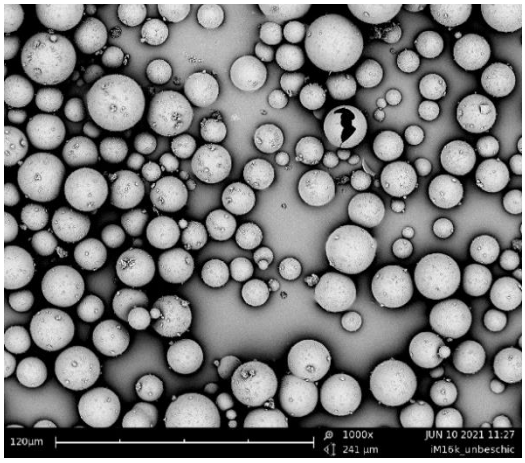

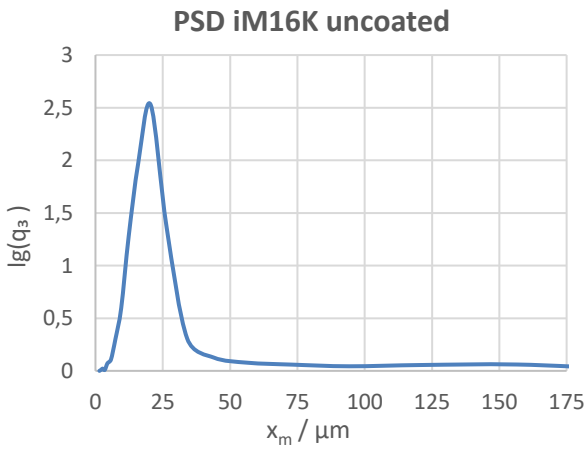

Figure 4: iM16K uncoated. SEM Picture on the left and particle size distribution on the right

The surface of the Cerabeads is significantly rougher compared to the Silibeads, as can be seen in the SEM image in figure 3. However, the surface is free of cracks. The particle morphology can be classified as spherical to slightly "potato-shaped". This is reflected in a value for the average sphericity of 0.823. Cerabeads have a larger average particle size compared to Silibeads. The D90

value of Cerabeads is 120.13 µm, which means that 10 % of the particles have a diameter which is bigger than the typical layer height of 120 µm. The high proportion of coarse particles potentially increases the surface roughness of laser-sintered components and could be problematic during processing.

The SEM images of the hollow glass spheres (iM16K uncoated) already show that they are much smaller than the other fillers (fig. 4). The D_{50} is 18.4 µm. For the most part, the glass spheres have an almost perfectly spherical shape. Under the scanning electron microscope, some broken glass bubbles can be seen. These have an uneven, flakey morphology. Smaller particles adhere to the surface of the hollow glass spheres, which can be seen well under higher magnification. The mean sphericity measured in the QICPIC is 0.829. This value is at disagreement with the spherical particle shape that can be seen by SEM and is possibly caused by the percentage of fractured glass. Due to the small particle size the powder flowability could be degraded by the addition of iM16K. Glass bubbles with a silane coating showed no obvious differences in terms of particle size distribution and particle morphology.

In addition to the particle morphology and the particle size distribution, the flowability of the powder is another important parameter to ensure a good powder layer application and a high powder bed density in the LS process. As already described, there are correlations between flowability, particle size distribution and particle morphology. In the scope of the investigations, the Hausner ratio was used to describe the flowability of powders and blends. If the Hausner ratio is below 1.25, the powder is supposed to have good flowability. With a ratio above 1.4, cohesion dominates and it is assumed that the powder tends to be unsuitable for the SLS process. Between a ratio of 1.25 and 1.4, the powder is classified as having limited flowability. [28]

The results for the powder flowability of dry blends in dependence on the filling ratio is given by figure 5. Starting with the results for PP based dry blends, it can be noted, that the addition of a filler materials with a filling ratio of 20 vol% improves the powder flowability for all tested fillers. Even hollow glass spheres (iM16K) improve the flowability compared to unfilled PP although they exhibited a worse flowability when tested separately. In contrast, the addition of 40 vol% of uncoated iM16K worsens the flowability. The greatest improvements can be achieved with the addition of 40 vol% Cerabeads or silane coated Silibeads. These fillers also showed the best flowability when measured separately. The Hausner ratio of the blends is below 1.25 in both cases, therefore the powder achieves a good flowability in contrast to the unfilled PP powder.

The results for PA613 based dry blends show the same trends as the results for PP (fig. 5). However, unfilled Vestosint PA613 has a better flowability when compared to PP. The influence of a 20 vol% filling ratio on the flowability is minor. All blends still have a good flowability. For a filling ratio of 40 vol%, the impact on the flowability is more pronounced. Silibeads and Cerabeads can again be used to slightly increase the flowability. Uncoated iM16K worsen the flowability to the point, where the powder is classified as having a reduced flowability. Again, the silane coated fillers tend to perform slightly better.

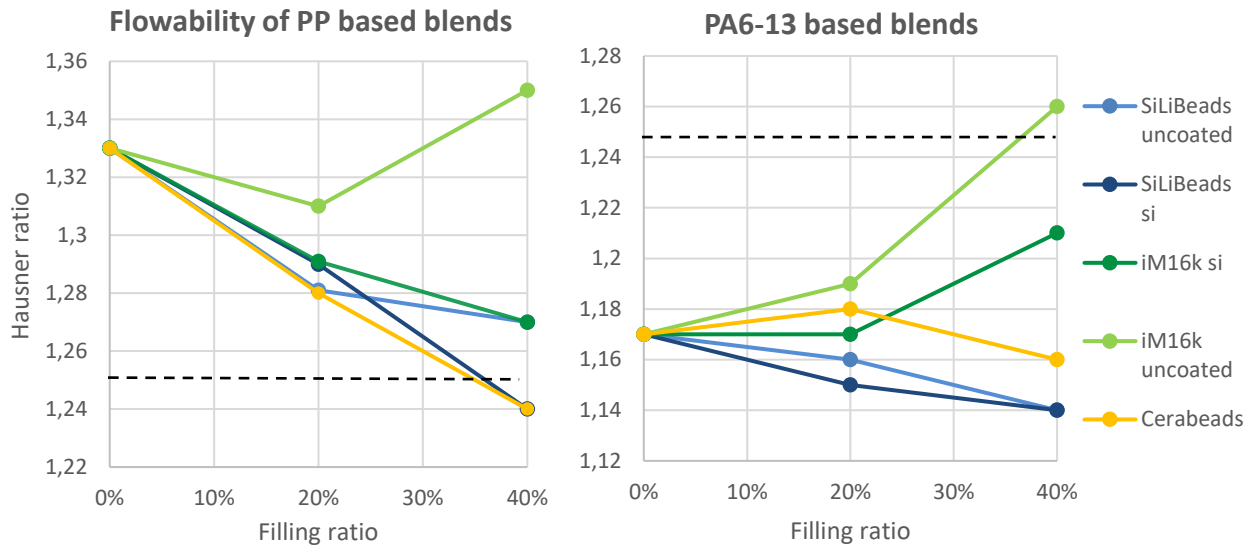

Figure 5: Hausner ratio of PP and PA613 based dry blends

In order to investigate the thermal behavior of the polymer powders and the powder blends, the respective temperature-process windows were determined by using DSC analyses. In addition to the effects on the temperature process window, other effects of the fillers on the heat capacity and the thermal conductivity of the powder bed are possible.

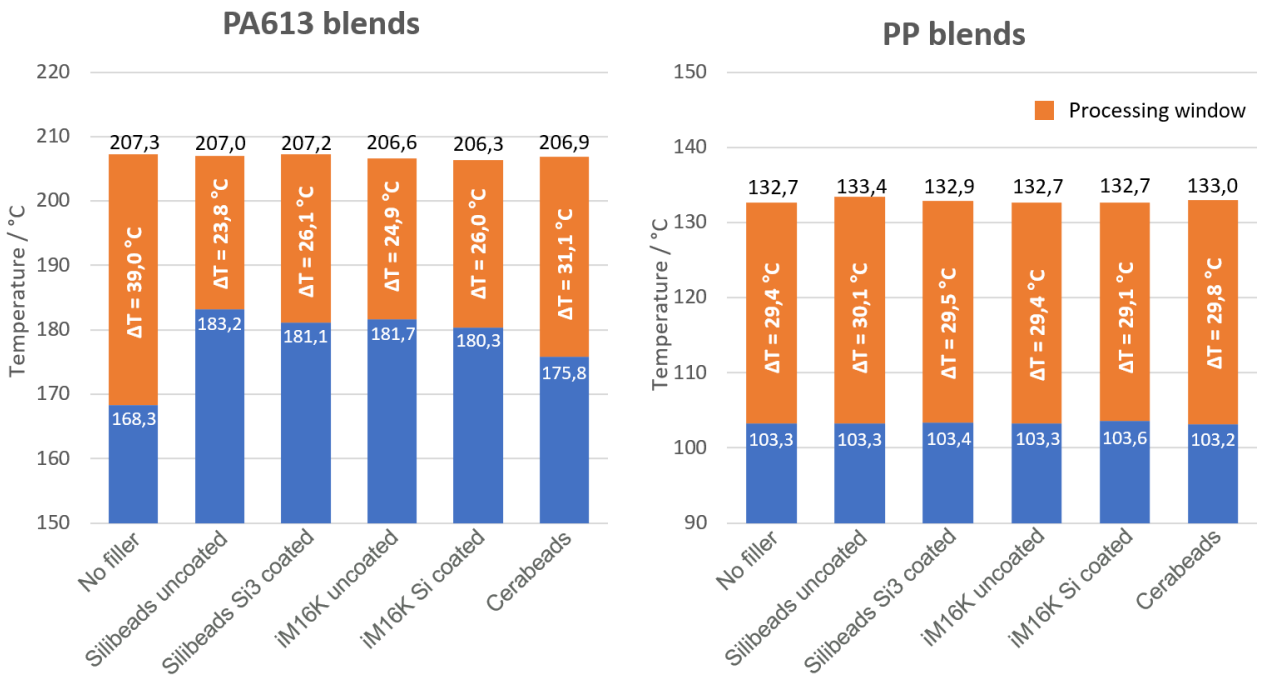

Figure 6: Thermal processing windows of PP and PA613 based dry blends with 40 vol% filler

The temperatures at the start of recrystallization and the start of the melting process have been extracted from the DSC curves and plotted in figure 6. At first glance, it can be seen that a narrowing of the process window takes place for all PA613 powder blends compared to unfilled

PA613. For all blends the start of the melting process remains unchanged compared to the unfilled material as expected. Only the recrystallization temperature is changed by the addition of fillers. Most likely fillers have a nucleating effect, which causes the PA613 crystals to grow earlier [14]. The process window for unfilled PA613 is around ΔT = 39 °C. The largest impact on the process window is observed for PA613 + 40 vol.% Silibeads uncoated. The processing window of the dry blend is narrowed to ΔT = 23.8 °C. The smallest impact on the processing window is observed for PA613 + Cerabeads 40 vol.%. The process window here has a span of ΔT = 31.1 °C. In the comparison between the silane coated and uncoated Silibeads and iM16k, respectively, the silanization seems to have a slightly positive effect on the size of the temperature process window.

In addition to the impact on the processing window a reduction in heat capacity and a reduction of the measured melting and recrystallization enthalpy were observed for the PA613 powder blends. The area under the peaks of the DSC curve is correspondingly smaller, since the filler does not melt and thus the enthalpy of melting of the mixture is lower. Heat capacity and thermal conductivity of polymer and filler are summarized in table 2.

The thermal processing windows for unfilled PP as well as for PP powder blends are also given by figure 6. In contrast to PA613, the fillers have no significant influence on the process window. Accordingly, the fillers do not seem to influence the recrystallization. A comparison of the coated and uncoated fillers also shows no difference. All the processing windows are at about ΔT ≈ 30 °C. Similar to PA613, a decrease of the heat capacity as well as a reduction of the area under the peaks in the heating and cooling curves could be observed for the PP powder blends.

Table 2: Thermal properties of base polymers and fillers

	Gravimetric Heat capacity [kJ/(kg*K)]	**Volumetric heat capacity** [J/(cm³*K)]	**Thermal conductivity** [W/(m*K)]	**Melting Enthalpy** [kJ/kg]
PA613 (Vestosint) [6]	1.70	0.82	0.23	106
PP (Ultrasint) [6]	2.00	0.82	0.20	78
Glass beads (Silibeads) [38]	0.75	1.09	1.00	-
Glass bubbles (iM16k) [38]	0.75	0.19	0.15	-
Mullite (Cerabeads) [26]	0.99	1.61	1.45	-

In summary, a clear influence of the filler on the thermal process window was found for PA613 blends. The reduction of the process window can correspondingly worsen the processing properties and cause build job failures due to curling. A new determination of the non-curl temperature is necessary in any case. At first glance, the addition of fillers has no effect on the thermal process window of PP blends. However, the addition of fillers changes the heat capacity and thermal conductivity of the powder. In laser sintering, the heat capacity of the powder in relation to its volume is particularly decisive, since the laser heats a volume element in order to melt it. The required laser power in the process is often specified as laser volume energy density. The relationship between volumetric c_{Vol} and gravimetric heat capacity c_{gra} is given by the powder bed density $\rho_{p,b}$.

$$c_{Vol} = c_{gra} * \rho_{p,b} \quad (1)$$

The energy required to melt a volume element E_V, neglecting heat losses to other volume elements, is given by the temperature difference before and after Laser interaction ΔT multiplied with the volumetric heat capacity of polymer $c_{Vol,P}$ and filler $c_{Vol,F}$ and the volumetric melting enthalpy $\Delta H_{M,vol}$. The filling ratio is accounted for by the factor V_f.

$$E_V = \Delta T * \left[c_{Vol,P} * (1 - V_f) + c_{Vol,F} * V_f\right] + \left(1 - V_f\right) * \Delta H_{M,vol} \quad (2)$$

With the aid of this equation, it is possible to estimate how the required laser energy volume density changes when processing dry blends. Glass hollow spheres, for example, have only about a quarter of the heat capacity of polymer powders and also do not absorb any melting enthalpy. It can therefore be estimated, that the required volumetric energy density will be reducing for an increasing filling ratio V_f. Cerabeads on the other hand have almost double the volumetric heat capacity of the polymer powders. This means that the required volumetric energy density can either increase or decrease depending on the temperature difference ΔT. In addition to the model-based differences in the required energy density, the differences in thermal conductivity have additional influences on the melting and cooling behavior of parts and therefore impact the processability.

The viscosity of the plastic melt is of great importance for the SLS process, since the molten particles must flow into each other without additional pressure being applied. Consequently, coalescence is based on surface tension, melt viscosity and gravitational force [3]. In order to characterize the flow behavior, MVR measurements were performed.

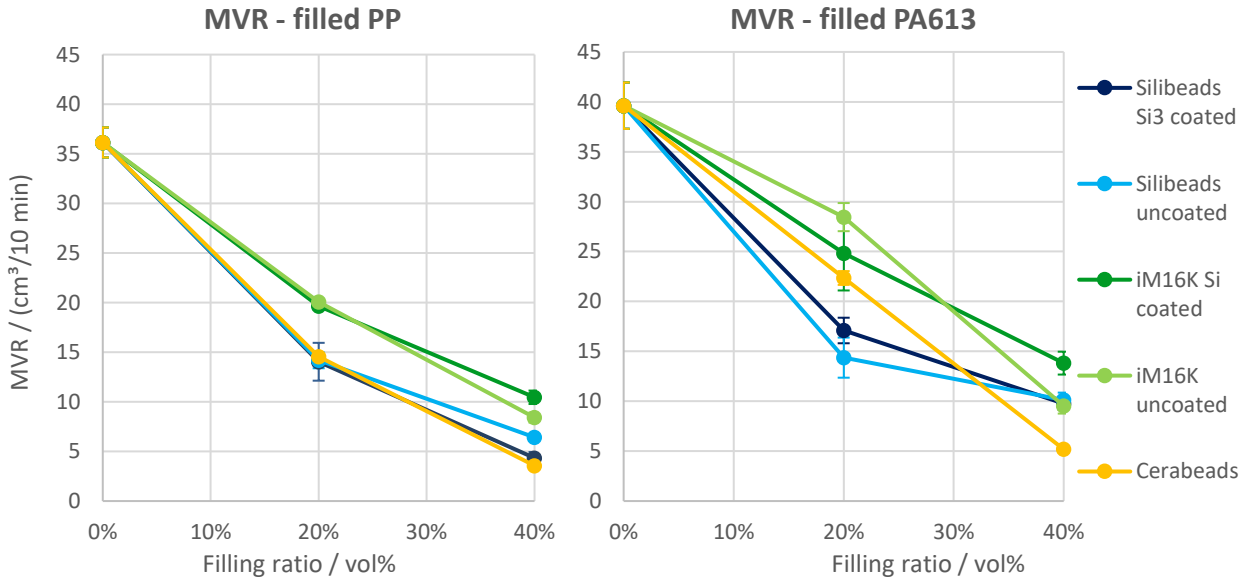

Figure 7: MVR values for powder blends depending on the filler content; test temperature for PP 220 °C and 240°C for PA613; test weight 5 kg; sample conditioning: 30 min at 105 °C

Figure 7 shows the impact of different fillers and filling ratios on the MVR-Value of PP and PA613 based dry blends. As expected, the addition of fillers generally lowers the MVR values since fillers do not melt and thus impair the flowability of the melt. For unfilled PP (mixed powder 60/40), the initial value at 220 °C test temperature and 5 kg test weight is 36.1 cm³/10min. By adding a volume fraction of 20 % filler, the MVR decreases to 14 – 20 cm³/10min. The MVR value further decreases to 4 – 10 cm³/10min if 40 vol% of filler is added. Cerabeads have the biggest

impact on the MVR value and the glass bubbles (iM16K) have the smallest impact. Furthermore, the silane coated variants of glass beads and glass bubbles tend to impact the MVR value slightly less compared to the uncoated variants. For PA12 powder, it is known that aged powder with a high viscosity tends to form surface defects such as “orange peel” [39]. In particular, for a high filling ratio a negative influence of the high MVR value on the component properties could be possible. However, it should be noted here, that the increase in viscosity observed in a nozzle flow for a filled polymer melt is not fully representative for the coalescence process upon laser sintering: This decrease in MVR, i.e. increase in macroscopic viscosity, is obtained while the viscosity of the matrix polymer is basically unchanged. Therefore, it is expected that the deterioration of the coalescence process is less than indicated by the reduced MVR.

For unfilled PA613 (virgin powder), the initial MVR value at 220 °C test temperature and 5 kg test weight is 39.6 cm³/10min. As already observed for PP blends, the melt volume flow rate decreases with increasing filler content. Again, glass bubbles (iM16K) had the smallest impact on the MVR values and Cerabeads had the largest impact at a filling ratio of 40 vol% decreasing the MVR value to only 5 cm³/10min. The differences between coated and uncoated variants of the same filler mostly fall in the range of the standard deviation for PA613 based blends and are therefore not significant. For both base materials, the influence of the filler on the MVR value decreases with decreasing filler diameter.

Parameter Development and Processability

The preliminary investigations on the powder have shown that the sintering window and the energy required to melt the powder can be changed by the addition of fillers. With regard to the powder flowability, only blends with hollow glass beads showed negative effects. Furthermore, the addition of fillers strongly reduces the MVR value. The essential parameters which are therefore adapted for the production of test specimens from dry blends are the build chamber temperature and the laser volume energy density.

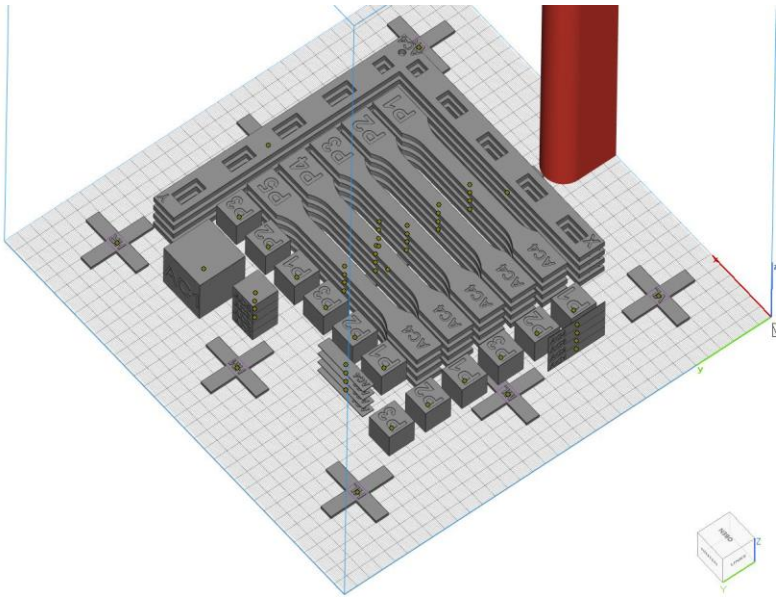

Figure 8: Build job layout for laser parameter development

Since the preliminary powder characterizations showed that the variants with silane coatings performed slightly better regarding relevant powder properties and additionally should provide better mechanical properties, the decision was made to focus on the coated variants. For each blend, initially the same build job was built to find suitable process parameters. The layout of this build job is shown in Figure 8.

For each blend, the first step was the determination of the non-curl temperature. For this purpose, the curl cross method was used. The build chamber temperature for unfilled PP is 138°C and for unfilled PA613 206.5 °C. If curling is detected for multiple curl crosses, the parts are removed, the build chamber temperature is increased by 2°C and a new attempt is made to build curl crosses. If only slight curling occurs for curl crosses in the corners of the build area, the temperature is increased by 1°C and a new set of curl crosses is built until none of the crosses showed visible signs of curling.

After determining a feasible build chamber temperature with the curl cross method, different test specimens are built with varying laser energy densities. To limit the number of variables and achieve parameters for a good machine productivity, the laser energy density is only varied by varying the laser power. The layer height is kept constant at 120 µm and the distance between two hatch lines is kept at 0.25 mm. The scan speed is kept constantly high at 4750 mm/s.

The selection of the best laser energy density is based on tensile strength, elongation at break, density, and a subjective assessment of resolution and surface quality. The tensile properties were determined in the dry state without conditioning the test specimens. These are only used to compare the different parameters, so conditioning is not necessary. The final mechanical properties will be presented later in figures 11 and 12.

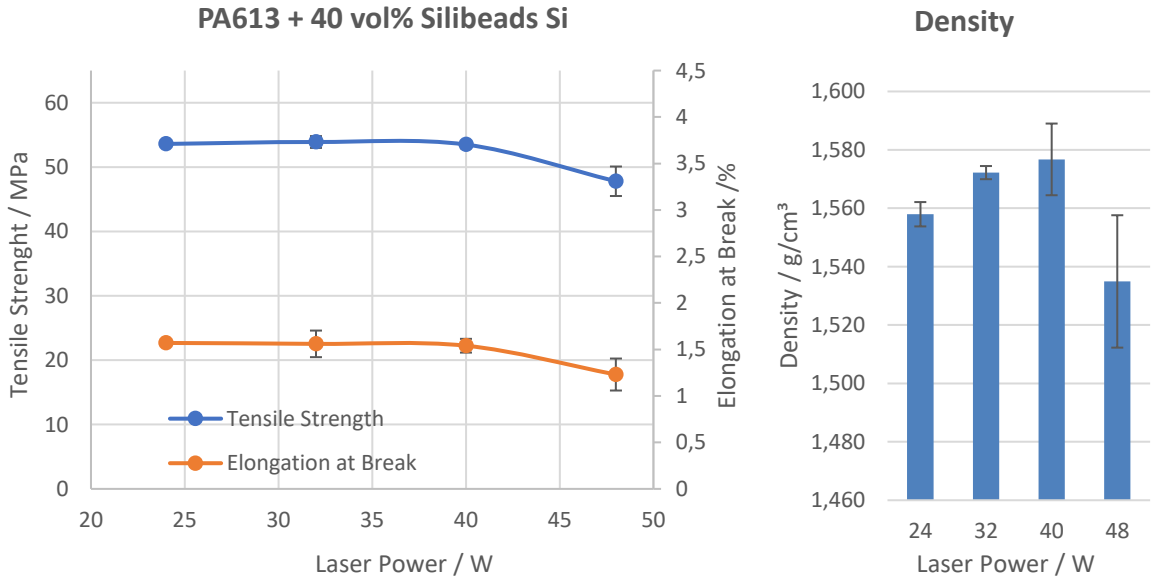

Figure 9: Mechanical properties and part density of PA613 with 40 vol% glass beads (Silibeads silane coated) in dependence of the laser power

Figure 9 plots tensile strength, elongation at break and density for different laser powers for a blend of PA613 with 40 vol% Silibeads with silane coating. It turns out that the mechanical properties of the blend remain almost the same for a relative wide range of laser powers. Looking at the mechanical properties only, laser energies ranging from 24 W to 40 W seem to be feasible for the given scan speed (4750 mm/s), hatch distance (0.25 mm) and layer height (0.12 mm). An optimal part density is achieved for 40 W laser power, however the value for 32 W is almost as good and showed less deviations.

The subjective evaluation of the component quality takes into account, among other things, the resolution of the marking, existing surface irritations, surface defects due to layer time jumps, but also the edge and corner quality. These variables were each given a quality rating of 1 to 5. Figure 10 shows the detail resolution and surface quality for PA613 blended with 40 vol% Silibeads Si3 coated. At first it can be noted that the addition of 40 vol% of glass beads gives the part a grayish color. Regarding the labeling, differences with increasing laser power are clearly visible. The letters and numbers are more precise at low laser power and degrade for the parameter set with higher laser power until they are barely recognizable at a laser power of 48 W. Furthermore, with increasing laser power, the effects of layer time jumps become visible, which negatively affects the resolution of the labeling (z-direction) of the density measurement cubes. The density cubes are particularly prone to surface defects in z direction since they have a relatively high volume and therefore cause a high local energy input. Additionally, with increasing laser power, a decrease in shape and dimensional accuracy with respect to corners and edges can be observed. In terms of component resolution, the parameters with a laser power of 24 W and 32 W were rated best.

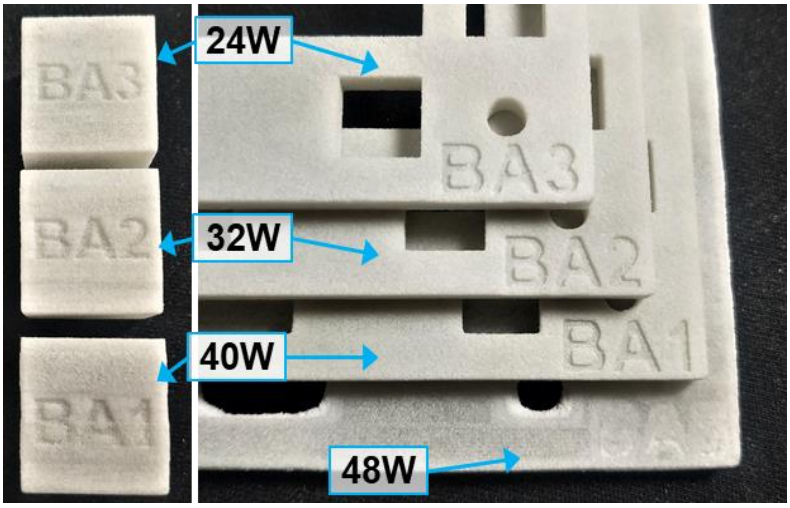

Figure 10: Part resolution and surface quality of PA613 with 40 vol% glass beads (Silibeads silane coated) in dependence of laser the power

Taking into account all the results (mechanical properties, density, resolution), it is found that the optimum laser energy for this blend is around 32 W. However, the results can be further optimized by varying other laser parameters and optimizing the contour exposure separately. Feasible exposure parameters were developed for all different dry blends using the same method.

Table 3: Processing parameters of PA613 based blends

PA613	unfilled	20 vol% Silibeads	40 vol% Silibeads	20 vol% iM16k	40 vol% iM16k	20 vol% Cerabead	40 vol% Cerabead
Bed temp. [°C]	206.5	206.5	206.5	207	208	206.5	209
Laser energy [W]	38	32	32	24	24	32	32

Table 4: Processing parameters of PP based blends

PP	unfilled	20 vol% Silibeads	40 vol% Silibeads	20 vol% iM16k	40 vol% iM16k	20 vol% Cerabead	40 vol% Cerabead
Bed temp. [°C]	138.5	138.5	138.5	140	142	139.7	-
Laser energy [W]	27.5	22	22	16,5	16.5	37	-

Mechanical Properties

The results for the PA613 based blends built with optimized parameters as described above are displayed in figure 11. First of all, it can be seen that with all fillers used, the stiffness in the dry state could be increased. With increasing filler content, the stiffness also increases. The highest increase can be achieved with the addition of 40 vol% Cerabeads. Here, the stiffness could be increased from 2162 MPa to 7550 MPa. The smallest increase in stiffness was obtained with the addition of the hollow glass beads. It can be assumed that the stiffness of the hollow spheres themselves is significantly lower than that of solid spheres, which means that the increase in Young's modulus is correspondingly lower.

At the same time, however, the elongation at break of PA613 blends decreases sharply with increasing filler content. Even at a filler volume fraction of 20%, the elongation at break for blends with hollow glass beads (iM16K) and Cerabeads is below 4% in the dry state. The addition of fillers has a less pronounced effect on the strength of PA613 blends in the dry state. While the strength remains almost constant with the addition of glass beads, it decreases slightly with increasing filler content of hollow glass beads and Cerabeads.

Comparing these results to the result after conditioning the samples, a massive impact of the moisture absorption especially for blends with PA613 and glass can be noticed. During conditioning, unfilled PA613 absorbs approx. 1.05 mass percent water. Depending on the filler, the blends absorb between 0.35 and 0.95 mass percent water. Due to the plasticizing effect of the water in PA613, the stiffness of the matrix decreases from 2162 MPa to 1507 MPa. The addition of 20 vol% Silibeads increases the modulus marginally to 1594 MPa. Increasing the filler content to 40 vol%, however, lowers the stiffness again. The addition of iM16K also causes only a slight increase in stiffness. The effect of conditioning on Cerabeads filled PA613 appears to be considerably less. Although the stiffness of these blends also decreases after conditioning, an increase in stiffness to 4850 MPa can be achieved with a filler content of 40 vol% Cerabeads.

Looking at the elongation at break after conditioning, it is first noticeable that there is an increase to almost 30% for unfilled PA613. This effect is also known and can be explained by the plasticizing effect of the water. The influence on the elongation at break of the blends is, however, even more pronounced. The elongation at break of PA613 with 40 vol% Silibeads with Si3 coating increases almost by a factor of 10 to 14% compared to the dry state. The elongation at break of the blend with Silibeads without coating increases even further.

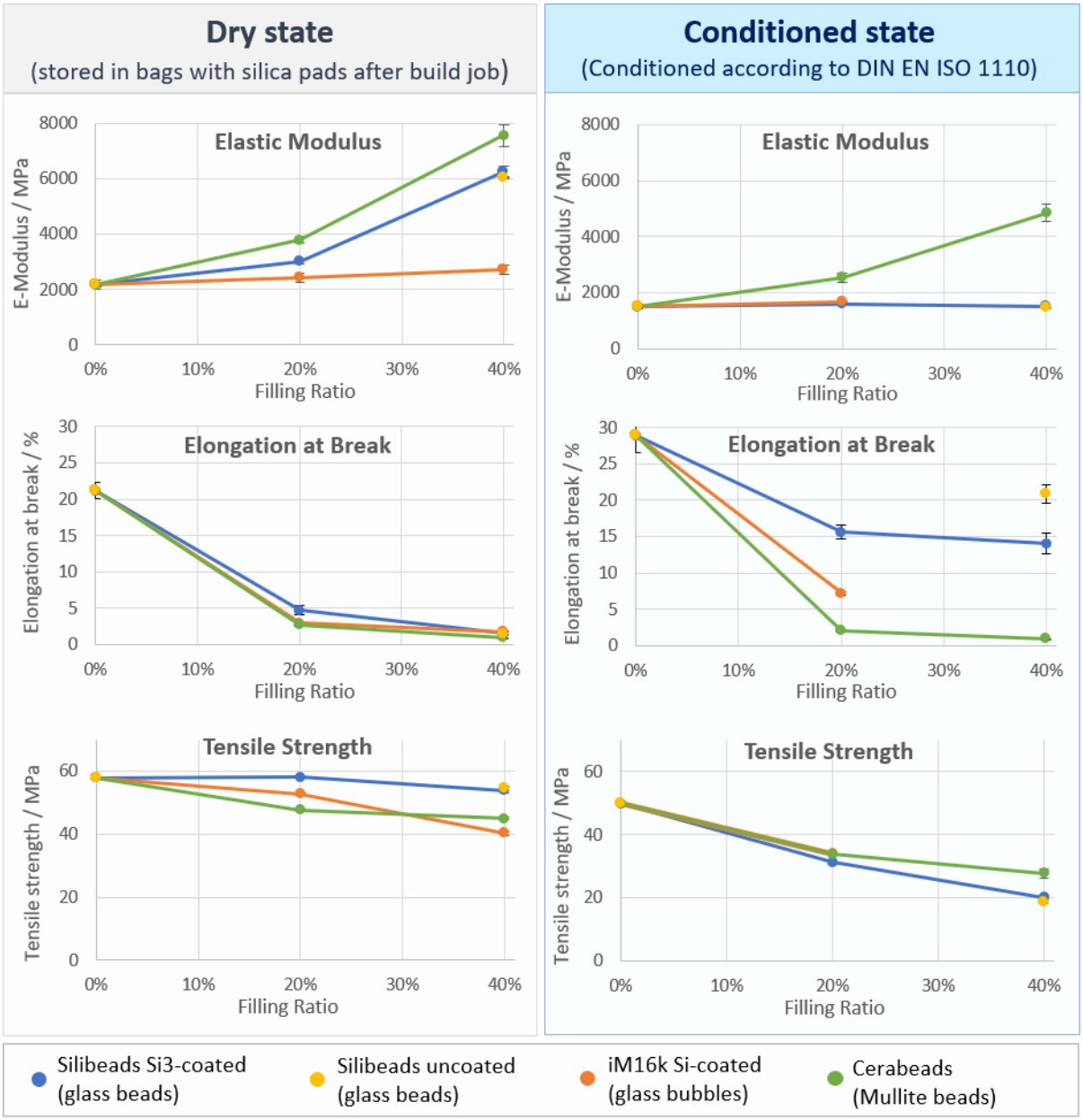

Figure 11: Mechanical properties of PA613 based dry blends build in X-direction

While the addition of 20 vol% Silibeads with Si3 coating had a positive effect on the strength of PA613 components, the strength of this blend drops significantly after conditioning. In

fact, the addition of 20 vol% Silibeads reduced the tensile strength of conditioned PA613 from 49.8 MPa to 31.2 MPa. As a simplification, it can be assumed that a filler content of 20 vol% reduces the cross-sectional area of the matrix by an average of 20 %. Due to the spherical shape of the fillers, however, this value fluctuates locally. Since the reduction in tensile strength due to the addition of 20 vol% glass beads is 35%, it can be assumed that the glass beads transmit almost no forces and that almost exclusively the matrix transmits the forces. The addition of 40 vol% glass beads deteriorates the tensile strength by approx. 60 %. There is no significant difference between uncoated glass beads and glass beads with silane coating. The tested silane coating therefore does not appear to be suitable for improving the adhesion between the glass beads and PA613 in laser-sintered components, especially since also no significant differences were found between the coated and uncoated glass beads. The tensile strength for blends with Cerabeads and iM16K decreased also after conditioning, but not to the same degree as the Silibeads. The adhesion was probably not degraded as much by conditioning. Potentially, the surface structure of the Cerabeads help to maintain better adhesion by providing some mechanical interlocking.

The only filler that can be classified as reasonable in combination with PA613 after the investigation of the mechanical properties are Cerabeads. At least if the components are to be used in a humid environment, dry blends of PA613 and glass lose their stiffness and strength. In addition to the plasticizing effect on the matrix, a degradation of the adhesion between polymer and filler was identified as the cause by analyzing SEM Images of the crack surfaces.

The results for the PP based blends are displayed in figure 12. Although the DIN EN ISO 1110 standard is actually only intended for polyamides and PP hardly absorbs any water, the PP tensile specimens were also tested in the dry state and after storage in a climatic chamber at 70°C and 62% relative humidity for 7 days. Even if the base polymer of the blend is hardly affected by the conditioning, the properties of the composite can still change if the fiber matrix adhesion is changed. Due to the poor processability of PP with Cerabeads as filler on EOS P3 systems, hardly any reliable data are available for this material combination.

Unfilled PP is significantly more ductile compared to PA613. The strength in the dry state is 28.9 MPa and the modulus of elasticity is 1316 MPa. The material achieves a nominal elongation at break of 41%. Again, the stiffness in the dry state can be increased by adding any of the fillers tested and, as for PA613, increases with increasing filler content. The largest increase in stiffness was obtained with 40 vol% Silibeads with Si3 coating. However, the elongation at break decreases strongly with increasing filler content. PP blends with a filler content of 20 vol% achieved good elongation at break between 8.7 % and 13.5 %, but they do not achieve the desired stiffness.

In contrast to PA613 blends, the strength of PP blends decreases significantly with increasing filler content even in the dry state. With the addition of 20 vol% filler, the hollow glass spheres achieve the best strength. For both glass hollow spheres and glass solid spheres, the strength drops to approx. 17 MPa at a filler volume fraction of 40%. This corresponds to a decrease of 40 % in strength and indicates that only low forces can be transmitted by the filler. The filler reduces the effective force-transmitting cross-section of the matrix under tensile load accordingly. The strength of all PP blends is below the values of PA613 blends. It has been shown that the lower strength of the PP cannot be increased by the addition of spherical fillers. This would require fillers with a large aspect ratio, which can achieve a corresponding strengthening effect.

The results after conditioning show that PP blends are also affected by moisture even though hardly any moisture absorption could be measured (< 0.02%). The influence on component stiffness is not as significant as for PA613. The Young's modulus of the blend with 20 vol% Silibeads drops from 1910 MPa to 1620 MPa after conditioning. At the same time, the strength decreases from 20.7 MPa to 16.5 MPa and the elongation at break increases from 11.5% to 25%.

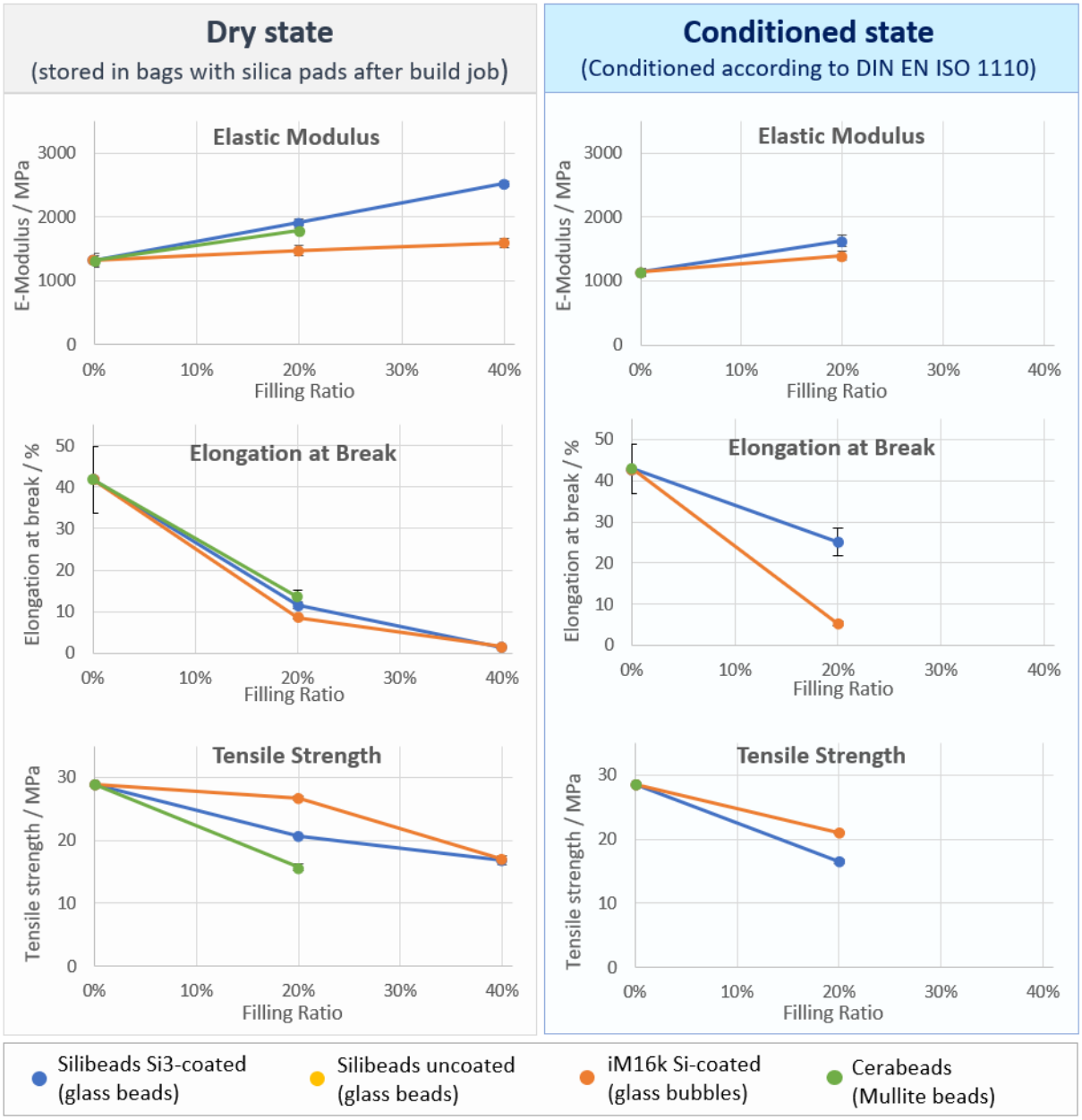

Figure 12: Mechanical properties of PP based dry blends build in X-direction

SEM images of the fracture surfaces of the tensile specimens are used to evaluate the adhesion between the filler and matrix. Ideally, the composite should fail in the matrix and not at the interfaces of filler and matrix. Accordingly, hardly any exposed filler without remaining plastic adhesions should be visible in the fracture surface. Exemplary, the fracture surfaces of PA613 with 20 vol% Silibeads with Si3 coating are investigated before and after conditioning (Figure 13).

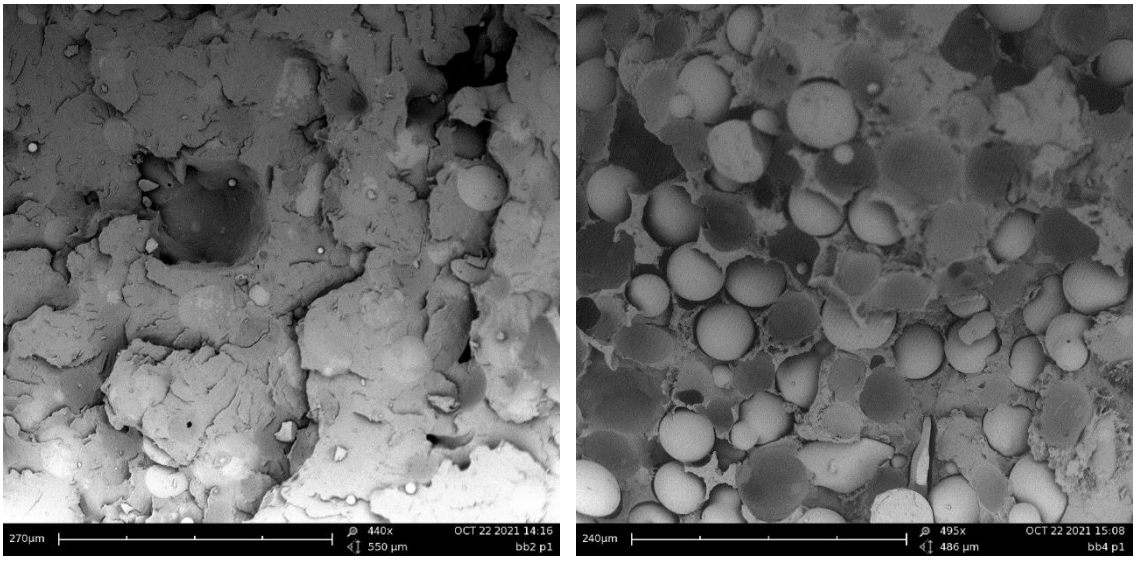

Figure 13: SEM crack surface. PA613 + 20 vol% Silibeads Si3 coated tested dry (left) and after conditioning (right)

The fracture surface after the tensile test in dry condition is shown on the left side. Only a few exposed glass spheres can be seen, and most glass spheres still have adherent plastic after the tensile test. The fracture surfaces of the polymer matrix show little deformation and an overall brittle fracture pattern. The glass beads are well embedded in the matrix, wetting with plastic in the LS process is consequently sufficiently good.

After the specimens have been conditioned at 70°C and 62% relative humidity for 7 days, their fracture pattern changes fundamentally. There are more exposed glass spheres to which no more plastic adheres. A gap to the plastic is clearly visible at the edge of the glass spheres. Since it could be concluded from the fracture surfaces of the specimens before conditioning that good wetting takes place in the LS process, it can be concluded that the plastic detaches from the glass during the tensile test. The glass spheres actually act as a defect. Obviously, almost no forces are transmitted by them. This also explains why the strength drops so significantly when glass beads are added in the conditioned state compared to the unfilled material. The polymer is stretched around the glass beads and has a more ductile failure mode. The silane coating of the glass beads does not seem to be suitable to ensure sufficient adhesion between matrix polymer and filler on laser sintered samples after conditioning until breakage. One assumption for explaining this effect is that water diffusing into the polyamide collects at the interfaces between filler and polymer. Due to its polarity, it can detach dipole interactions between polyamide molecules and the glass surface.

Summary

The investigations showed that dry blending of spherical micro fillers into LS powder can influence the relevant processing properties. In addition to an increased melt viscosity, the change in the thermal properties of the powder is particularly relevant to the process. For this purpose, a concept was presented to adapt the laser power and the build chamber temperature specifically for different powder mixtures. Furthermore, it was shown that the component stiffness can be deliberately increased by the addition of spherical fillers. However, the elongation at break

decreases in the process. When testing conditioned tensile specimens, it was found that the mechanical properties of PA613 blends with glass in particular are strongly influenced by moisture absorption. Besides the plasticizing effect of moisture on the PA, a deterioration of the filler-matrix adhesion was identified as the cause. Adhesion between PA and Cerabeads was affected less by the influence of water. Accordingly, the silane coatings of the glass fillers could not effectively prevent the loss of adhesion. Further investigations on the improvement of the adhesion between filler and plastic in the LS process will be carried out at the DMRC in the future.

References

[1] Wohlers Associates, Ed., *3D Printing and Additive Manufacturing State of the Industry: Anual Worldwide Progress Report*. Colorado: WOHLERS ASSOCIATES INC., 2018.

[2] Sculpteo, *The Sate of 3D Printing: 2021 Edition.* [Online]. Available: https:// www.sculpteo.com/de/ebooks/state-of-3d-printing-report-2021/ (accessed: Dec. 9 2021).

[3] M. Schmid, *Selektives Lasersintern (SLS) mit Kunststoffen*. München: Hanser, 2015.

[4] L. J. Tan, W. Zhu, and K. Zhou, "Recent Progress on Polymer Materials for Additive Manufacturing," *Adv. Funct. Mater.*, vol. 30, no. 43, p. 2003062, 2020, doi: 10.1002/adfm.202003062.

[5] M. Xanthos, *Functional Fillers for Plastics*. Weinheim: Wiley, 2005.

[6] E. Baur, S. Brinkmann, T. A. Osswald, N. Rudolph, E. Schmachtenberg, and H. Saechtling, *Saechtling Kunststoff Taschenbuch,* 31st ed. München: Hanser, 2013.

[7] W. Kaiser, *Kunststoffchemie für Ingenieure: Von der Synthese bis zur Anwendung,* 5th ed. München: Hanser, 2021. [Online]. Available: https://www.hanser-elibrary.com/doi/book/ 10.3139/9783446466029

[8] Y. Wang, J. Shen, M. Yan, and X. Tian, "Poly ether ether ketone and its composite powder prepared by thermally induced phase separation for high temperature selective laser sintering," *Materials & Design*, vol. 201, p. 109510, 2021, doi: 10.1016/j.matdes.2021.109510.

[9] A. A. Mousa, D. T. Pham, and S. P. Shwe, "Preprocessing studies for selective laser sintering of glass beads-filled PA12," *IJRAPIDM*, vol. 4, no. 1, p. 28, 2014, doi: 10.1504/IJRAPIDM.2014.062036.

[10] R. G. Kleijnen, J. P. W. Sesseg, M. Schmid, and K. Wegener, "Insights into the development of a short-fiber reinforced polypropylene for laser sintering," in *AIP Conference Proceedings*, Lyon, France, 2017, p. 190002. [Online]. Available: https://aip.scitation.org/ doi/pdf/10.1063/1.5016791

[11] J. Kim and T. S. Creasy, "Selective laser sintering characteristics of nylon 6/clay-reinforced nanocomposite," *Polymer Testing*, vol. 23, no. 6, pp. 629–636, 2004, doi: 10.1016/j.polymertesting.2004.01.014.

[12] P. Forderhase, K. McAlea, and R. Booth, "The Development of a SLS Plastic Composite Material," in *SFF Symposium Preceedings 1995*, Austin, 1995, pp. 287–297.

[13] H. Chung and S. Das, "Processing and properties of glass bead particulate-filled functionally graded Nylon-11 composites produced by selective laser sintering," *Materials Science and Engineering: A*, vol. 437, no. 2, pp. 226–234, 2006, doi: 10.1016/j.msea.2006.07.112.

[14] C.-Z. Yan, Y.-S. Shi, J.-S. Yang, and L. Xu, "Preparation and Selective Laser Sintering of Nylon-12-Coated Aluminum Powders," *Journal of Composite Materials*, vol. 43, no. 17, pp. 1835–1851, 2009, doi: 10.1177/0021998309340932.

[15] K. Wudy, L. Lanzl, and D. Drummer, “Selective Laser Sintering of Filled Polymer Systems: Bulk Properties and Laser Beam Material Interaction,” *Physics Procedia*, vol. 83, pp. 991–1002, 2016, doi: 10.1016/j.phpro.2016.08.104.
[16] B. Chen, S. Berretta, R. Davies, and O. Ghita, “Characterisation of carbon fibre (Cf) - Poly Ether Ketone (PEK) composite powders for laser sintering,” *Polymer Testing*, vol. 76, pp. 65–72, 2019, doi: 10.1016/j.polymertesting.2019.03.011.
[17] J. Schmidt *et al.,* “A novel process route for the production of spherical SLS polymer powders,” in Cleveland, Ohio, USA, 2015, p. 160011.
[18] P. Snarr, J. Beaman, and D. Haas, “Investigating Thermally Induced Phase Separation as a Composite Powder Synthesis Technique for Indirect Selective Laser Sintering,” in *Solid Freeform Fabrication 2021: Proceedings of the 32nd Annual International*, Solid Freeform Fabrication Symposium, Ed., 2021, pp. 678–687.
[19] BASF, *Technical Data Sheet Ultrasint® PP nat 01.* [Online]. Available: https://forward-am.com/material-portfolio/ultrasint-powders-for-powder-bed-fusion-pbf/pp-line/ultrasint-pp-nat-01/ (accessed: May 19 2021).
[20] C. Kummert, W. Diekmann, K. Tews, and H.-J. Schmied, “Influence of Part Microstructure on mechanical Properties of PA6X Laser Sintered Specimens,” in *Solid Freeform Fabrication 2019 - Proceedings*, Laboratory for Freeform Fabrication and University of Texas at Austin, Ed., 2019, pp. 735–744.
[21] R.-D. Maier and M. Schiller, Eds., *Handbuch Kunststoff-Additive,* 4th ed. München: Hanser, 2016.
[22] S. Arai, S. Tsunoda, A. Yamaguchi, and T. Ougizawa, “Characterization of flame-retardant poly(butylene terephthalate) processed by laser sintering,” *Optics & Laser Technology*, vol. 117, pp. 94–104, 2019, doi: 10.1016/j.optlastec.2019.04.006.
[23] A. Jansson and L. Pejryd, “Characterisation of carbon fibre-reinforced polyamide manufactured by selective laser sintering,” *Additive Manufacturing*, vol. 9, pp. 7–13, 2016, doi: 10.1016/j.addma.2015.12.003.
[24] Sigmund Lindner, *Silibeads Solid: durable and resilient products.* [Online]. Available: https://www.sigmund-lindner.com/wp-content/uploads/2018/09/SiLibeads_Solid_de.pdf (accessed: Jan. 6 2022).
[25] 3M Advanced Materials Division, *3M™ Glass Bubbles: Start something big, by thinking small.* [Online]. Available: https://www.3mdeutschland.de/3M/de_DE/p/d/b40064613/ (accessed: 007.01.2022).
[26] ITOCHU CERATECH Corp., *Naigai Cerabeads 60.* [Online]. Available: http://www.itc-cera.co.jp/english/prod/index.html (accessed: Sep. 17 2021).
[27] *Particle size analysis — Image analysis methods — Part 2: Dynamic image analysis methods*, 13322-2, ISO, 2021.
[28] *Additive Fertigungsverfahren Laser-Sintern von Kunststoffbauteilen Materialqualifizierung*, 3405 Blatt 1.1, VDI, Berlin, 2018.
[29] *Kunststoffe – Dynamische Differenz-Thermoanalyse (DSC) – Teil 3: Bestimmung der Schmelz- und Kristallisationstemperatur und der Schmelz- und Kristallisationsenthalpie*, 11357-3, DIN EN ISO, Berlin, 2018.
[30] *Kunststoffe – Bestimmung der Schmelze-Volumenfließrate (MVR) und Schmelze-Massefließrate (MFR) von Thermoplasten*, 1133, DIN EN ISO, Berlin, 2009.
[31] *Kunststoffe – Verfahren zur Bestimmung der Dichte von nicht verschäumten Kunststoffen – Teil 1: Eintauchverfahren, Verfahren mit Flüssigkeitspyknometer und Titrationsverfahren*, 1183-1, DIN EN ISO, Berlin, 2019.

[32] Sartorius, *CPA Analysenwaage.* [Online]. Available: https://www.sartorius.com/shop/ww/de/eur/produkte-labor-lab-products-and-services-accessories-and-consumables/cpa-analysenwaage/p/CPA224S# (accessed: Jan. 7 2022).
[33] *Kunststoffe - Bestimmung der Zugeigenschaften*, 527, DIN EN ISO, Berlin, 2019.
[34] *Kunststoffe – Polyamid (PA)-Formmassen für das Spritzgießen und die Extrusion – Teil 2: Herstellung von Probekörpern und Bestimmung von Eigenschaften*, 16392-2, DIN EN ISO, Berlin, 2017.
[35] *Kunststoffe – Polypropylen (PP)-Formmassen – Teil 2: Herstellung von Probekörpern und Bestimmung von Eigenschaften*, 19069-2, DIN EN ISO, [Heidelberg], 2020.
[36] *Kunststoffe – Polyamide – Beschleunigte Konditionierung von Probekörpern*, 1110, DIN EN ISO, Berlin, 2019.
[37] Y. Shi, Z. Li, H. Sun, S. Huang, and F. Zeng, "Effect of the properties of the polymer materials on the quality of selective laser sintering parts," *Proceedings of the Institution of Mechanical Engineers, Part L: Journal of Materials: Design and Applications*, vol. 218, no. 3, pp. 247–252, 2004, doi: 10.1177/146442070421800308.
[38] P. Stephan, S. Kabelac, M. Kind, D. Mewes, K. Schaber, and T. Wetzel, *VDI-Wärmeatlas*. Berlin, Heidelberg: Springer Berlin Heidelberg, 2019.
[39] S. Rüsenberg, "Prozessqualifizierung zur verlässlichen Herstellung von Produkten im Polymer Lasersinterverfahren," Dissertation, Universität Paderborn, Shaker Verlag, 2015.